

Gasoline Direct Injection Compression Ignition (GDCI) - Diesel-like Efficiency with Low CO₂ Emissions

2011-01-1386

Published
04/12/2011Mark Sellnau, James Sinnamon, Kevin Hoyer and Harry Husted
Delphi Corporation

Copyright © 2011 SAE International

doi:10.4271/2011-01-1386

ABSTRACT

A single-cylinder engine was used to study the potential of a high-efficiency combustion concept called gasoline direct-injection compression-ignition (GDCI). Low temperature combustion was achieved using multiple injections, intake boost, and moderate EGR to reduce engine-out NO_x and PM emissions engine for stringent emissions standards. This combustion strategy benefits from the relatively long ignition delay and high volatility of regular unleaded gasoline fuel.

Tests were conducted at 6 bar IMEP - 1500 rpm using various injection strategies with low-to-moderate injection pressure. Results showed that triple injection GDCI achieved about 8 percent greater indicated thermal efficiency and about 14 percent lower specific CO₂ emissions relative to diesel baseline tests on the same engine. Heat release rates and combustion noise could be controlled with a multiple-late injection strategy for controlled fuel-air stratification. Estimated heat losses were significantly reduced. GDCI has good potential for full-time operation over the US Federal drive cycle.

INTRODUCTION

Compression-ignited diesels have long been the most efficient internal combustion engines. However, diesel engines are challenged to meet future stringent NO_x and PM emissions regulations at acceptable cost. Kalghatgi demonstrated in both large bore [1,2] and small bore diesel engines [3] that if gasoline-like fuels are injected near but before TDC, both very low NO_x and PM emissions, and high efficiency, could be achieved. This combustion process may be described as “premixed enough” but not “fully mixed,” as

in homogeneous charge compression ignition (HCCI) engines.

Kalghatgi [4] showed that the higher resistance to autoignition for the gasoline fuels means these fuels have greater ignition delay than the diesel mid-distillate fuels. [Figure 1](#) shows octane number plotted against volatility for a range of fuel types [4]. During the injection and mixing processes, gasoline fuels have more time for fuel-air mixing. The higher volatility of gasoline also aids in the mixing process. This established that gasoline fuels including alcohols are better suited for partially premixed, low-temperature combustion processes.

Groups at the University of Wisconsin [5,6,7] and Lund University [8,9,10] have also tested gasoline fuels in diesel engines. They demonstrated high-load capability using gasoline and ethanol in both heavy-duty and light-duty diesel engines. Extensive computational studies were conducted by Ra and Reitz [7]. Predicted cylinder pressure, heat release, and emissions for gasoline injection were compared to those for diesel injection. Both single and double injection strategies with various injection timings were investigated to achieve minimum emissions. With this previous work, it is evident that operation of CI engines on gasoline fuels can greatly facilitate low NO_x and low smoke operation. These studies demonstrated good potential for high load operation beyond typical HCCI levels.

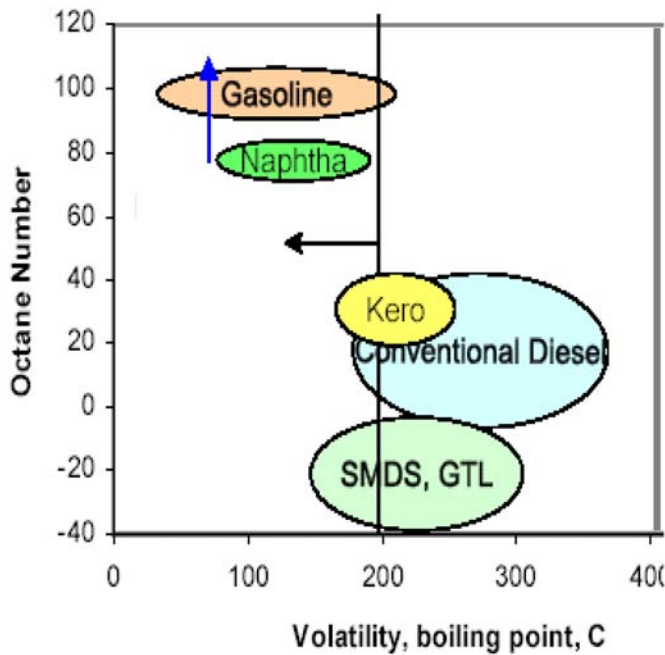


Figure 1. Octane number as a function of volatility for a range of fuel types from reference [4].

All of these prior studies have been conducted on production diesel engines with diesel fuel injection systems. Many issues remain related to light load operation, injection strategies and injection pressure requirements, control of pressure rise rates, combustion noise, high speed operation, and cold starting. Practical system implementation has not been demonstrated.

In the current work, the combustion process is referred to as Gasoline Direct Injection Compression Ignition (GDCI). Preliminary single-cylinder engine tests were performed at a medium speed and medium load condition. One objective is to achieve GDCI combustion using low injection pressures below the typical diesel range. A GDCI injection system is being developed for this purpose. Various injection strategies were tested and evaluated against preliminary emissions targets and noise constraints.

EXPERIMENTAL DESCRIPTION

The experiments performed in this study were performed on a Ricardo Hydra light-duty single-cylinder engine. A photograph of the engine is shown in [Figure 2](#); dimensions for the engine are listed in [Table 1](#). The engine configuration is four-valve, double-overhead cam with central injection. The aluminum cylinder head is rated at 200 bar peak cylinder pressure (PCP).

The engine is very flexible and parts can be easily interchanged. A removable injector sleeve enables testing of various injector types and sizes. Valve events may be changed by changing camshafts. Pistons and piston shapes

can also be changed and compression ratio adjusted via block shims. A port throttle on the rear intake port regulates the in-cylinder swirl ratio between 0.5 and 3.0.

The fuel used was regular unleaded RON91 gasoline representative of available pump fuel in the United States. The fuel contained no oxygenates. Fuel properties are shown in [Table 2](#).

The fuel injection system used was a Delphi developmental gasoline direct-injection system. Fuel pressure at the injector inlet was measured using a Kistler 4067C dynamic pressure transducer.

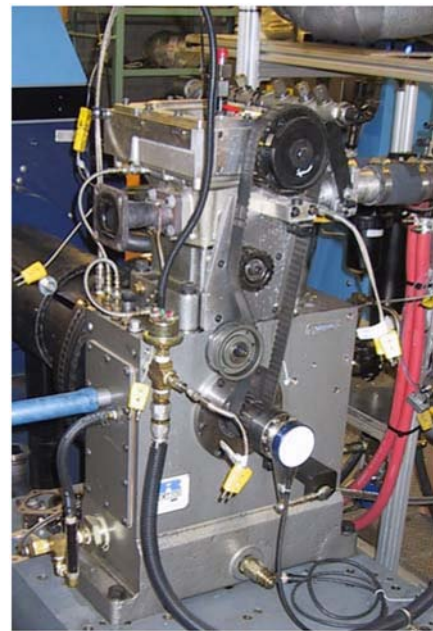


Figure 2. Single-cylinder Hydra engine.

Table 1. Specifications and dimensions of single-cylinder Hydra test engine.

Engine Type	4-valve Comp. Ignition
Bore × Stroke	84 × 90 mm
Displacement	499 cc
Compression Ratio	16.2 (adjustable)
Max. Cyl. Pressure	200 bar
Injection	Central mount – various injector types
Piston & Bowl	piston blanks & variants
DOHC Type II Valvetrain	Fixed cams (selectable)
Swirl ratio	Variable (0.5 ~ 3.0) PDA

A schematic diagram of the engine test setup is shown in Fig. 3. The intake and exhaust systems allowed simulated turbo-charged operation with wide range of intake and exhaust pressures. The intake air temperature was controlled using a 6 kW Chromalux air heater. EGR was controlled by a V-cut ball valve located between the exhaust and intake surge tanks. EGR was cooled by a water-cooled heat exchanger. Two 38 liter tanks were used as the intake and exhaust surge tanks in order to minimize pressure fluctuations and to mix the EGR well with the fresh intake air.

Air flow was controlled and measured with a Flow Systems FC-500 air system using a 7-nozzle sonic array. Fresh and dry air was supplied from the building compressed air system. Regulation of intake air to the engine was very good.

Fuel flow was measured with a high-precision Pierburg PLU103b fuel meter. The total error of this instrument as calibrated is 0.3 percent of reading down to 0.05 g/s fuel flow. This provided very accurate measurements of fuel flow to the engine even at idle conditions.

All emissions were measured on a wet basis using heated sampling systems with filters at 191 deg C. An AVL Sesam FTIR was used for carbon species, nitrogen species, and some hydrocarbon species. A Horiba Fast FID was used for total hydrocarbon emissions, and a Rosemount MLT-3 was used for exhaust oxygen and intake CO₂ emissions. An AVL 415S smoke meter was used to measure particulate emissions.

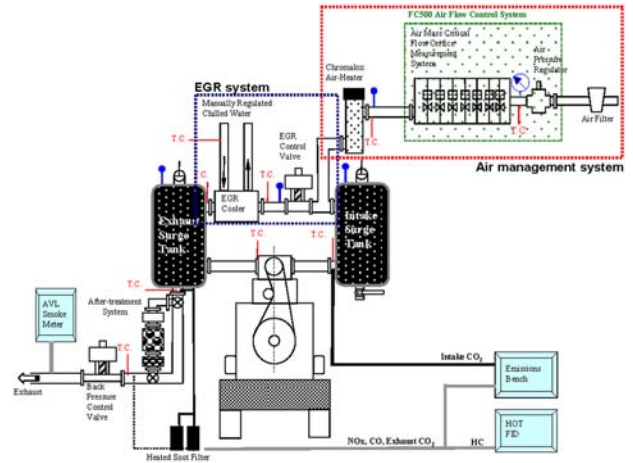


Figure 3. Schematic diagram of engine setup.

Cylinder pressure was measured with a flush-mounted Kistler 6125CU20 pressure transducer. A Kistler 2613B crankshaft encoder provided crank position data and was dynamically aligned with engine TDC using a Kistler 2629B TDC probe. Pressure data was sampled every 0.5 CAD.

A single-cylinder engine controller was developed with real-time heat release analysis capability. A schematic of the controller with sensors and actuators is shown in Figure 4. Both high-speed and low-speed data may be acquired by the system. The controller is based on National Instruments hardware and Labview software [11], and was built by Drivven, Inc [12].

Residual mass concentration in the cylinder was measured by a Delphi Residual Estimator Tool (RET) [13, 14]. Figure 5 shows the RET. Inputs to the RET are cylinder pressure, average intake and exhaust port temperatures, and average intake and exhaust pressures.

Table 2. Fuel properties for test gasoline.

Parameter	Value	Units
Density	0.7426	g/cc
H/C Ratio	1.871	atomic
O/C Ratio	0	atomic
Lower Heating Value	43.397	MJ/kg
Octane	86.65	
RON	90.6	
MON	82.7	
T0	33.8	C
T50	99.2	C
T100	209.2	C
Aromatics	26.1	vol%
Olefins	2.8	vol%
Saturates	70.9	vol%
Ethanol	0	vol%
Sulfur	5	ppm

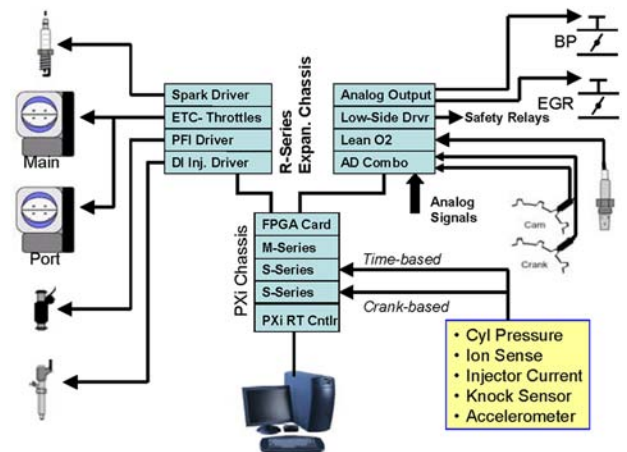


Figure 4. Schematic of test cell single-cylinder engine controller with real-time heat release analysis.

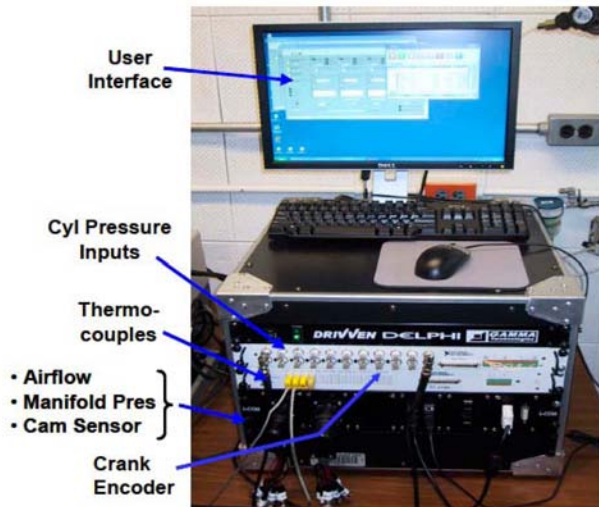


Figure 5. Residual Estimator Tool (RET).

METHODOLOGIES: TEST AND ANALYSIS

The injection process is very important to achieve the necessary fuel-air mixing and stratification control for GDCI combustion. Injection characteristics need to be developed systematically to minimize fuel consumption and emissions within system constraints such as combustion noise. Low injection pressure is desired to keep cost of injection system low and reduce fuel pump parasitics.

Fuel injection parameters are defined in Figure 6, where SOI1 to SOI5, Q1 to Q5 and PW1 to PW5 are the start-of-injection timings in crank angle degrees (CAD), injection quantities in cubic millimeters, and injector driver pulse-widths in milliseconds, respectively, for each of five injection events. Knowledge of the injection quantity is required for each injection event; however, both rail pressure and cylinder pressure are time-varying. Injection pressure pulsations induced by each pulse have a significant effect on fuel quantity delivered by subsequent pulses. This makes it impossible to simply determine injection quantities from average rail pressure, injection PW, and the injector calibration map.

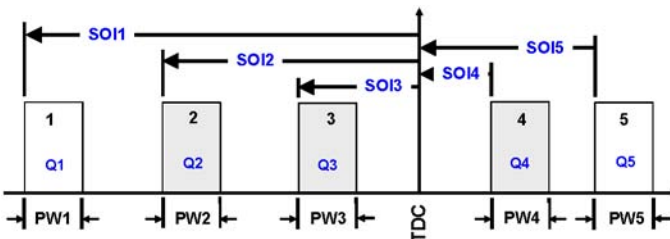


Figure 6. Injection parameter definitions.

Multiple-Injection Control Utility

A multiple-injection control utility that compensates for the effects of rail pressure pulsations was developed and implemented in the test cell engine controller using Labview [11]. It is shown schematically in Figure 7.

The user inputs are the SOI timings, the fractions of total fuel delivery, $Q\%$, and the desired engine IMEP. The measured inputs are IMEP from the cylinder pressure transducer, measured total fuel quantity from the fuel meter, crank-angle-resolved cylinder pressure and crank-angle-resolved injection pressure measured using a transducer located near the injector inlet. By processing the cylinder and injection pressure signals, with an embedded injector calibration, the required pulse-widths are determined. The algorithm also modulates commanded total Q for closed-loop PID control of IMEP to the desired test value while maintaining the desired fuel fractions for each injection. Similarly, closed-loop PID control of intake and exhaust pressure, injector rail pressure, EGR, and intake air temperature is used to improve speed and accuracy in setting engine test points.

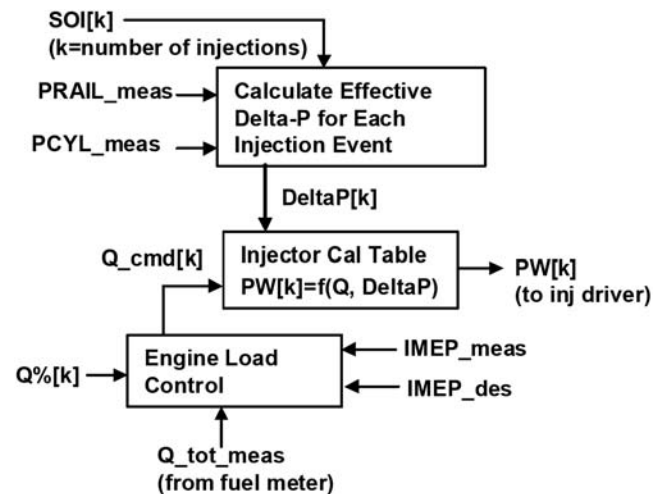


Figure 7. Multiple-injection pulse-width control with closed-loop IMEP control.

Design of Experiments, Response Surface Modeling and Optimization

The number of injection parameters is too large to permit use of traditional parametric test methods. Therefore state-of-the-art methods for design of experiments (DoE), response surface modeling (RSM) and optimization were applied. The model-based control (MBC) toolbox from Mathworks, Inc. [15] was used for this purpose.

Figure 8 shows a Stratified Latin Hypercube DoE design used to examine the effects of injection parameters with a triple-injection strategy. There are five “global” DoE variables. At

each DoE point an injection timing hook using SOB was performed. SOB is called a “local” variable.

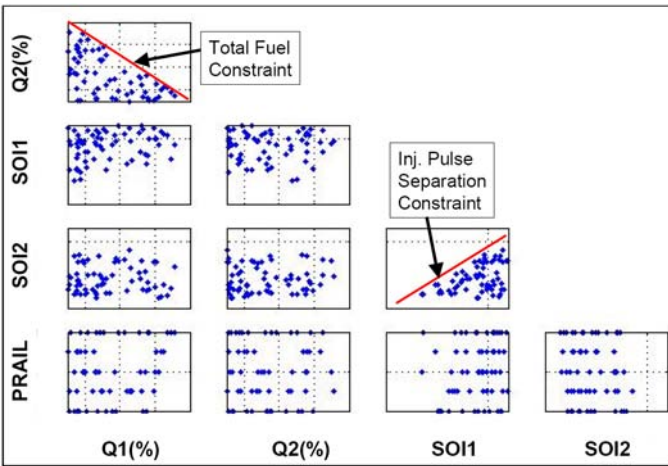


Figure 8. DoE design space for triple-injection tests.

Constraints have been applied to limit the points to encompass only the possible combinations of Q1 and Q2 while meeting the desired engine IMEP. Similarly a minimum pulse-separation constraint is applied to SOI. Injection timing and quantities are assigned using space-filling techniques as shown in Figure 8.

Guidelines for the minimum number of test points needed to fit a high-quality response surface model (RSM) have been developed. For the case shown, with five global variables, approximately 50 points are required. In the case shown here, the DoE has 65 points, of which 48 were actually acquired in testing. At each global point approximately 3 or 4 local (SOB) points were obtained for a total of 167 test points.

RSMs were fit using all six independent variables and constrained optimization was performed. Figures 9 and 10 show modeling and optimization results for 1500 RPM, 6 bar IMEP with triple-injection. In this case, optimization constraints for FSN<0.5, and CNL<85 dBA and Prail<500 bar were applied. The surface plot shows ISFC against injection quantities with injection timings and injection pressure set at their optimized values. The model is valid within the colored region while the pale yellow region represents extrapolation beyond the data boundary. The cross-section view in Figure 10 is more informative. The trends with respect to each of the independent variables are shown about a set-point (chosen by the user) represented by the vertical orange lines. In the case shown, the set-point is at the optimized operating condition. Again, yellow regions represent extrapolation outside the data boundary.

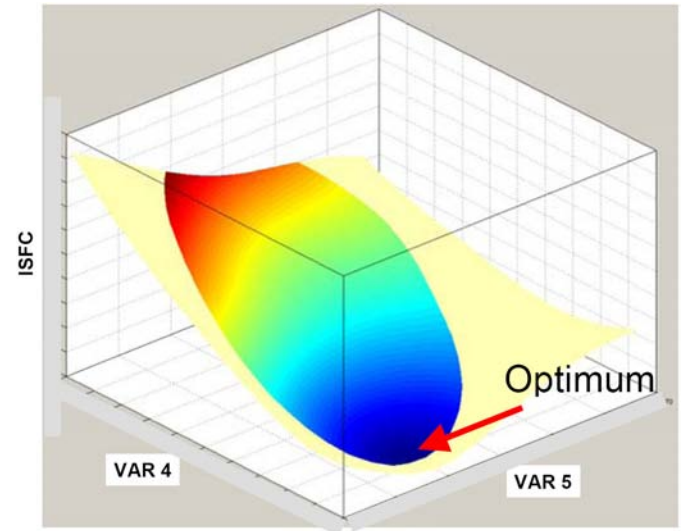


Figure 9. Response Surface Model for ISFC, 1500 RPM, 6 bar IMEP, using Triple Injection Strategy

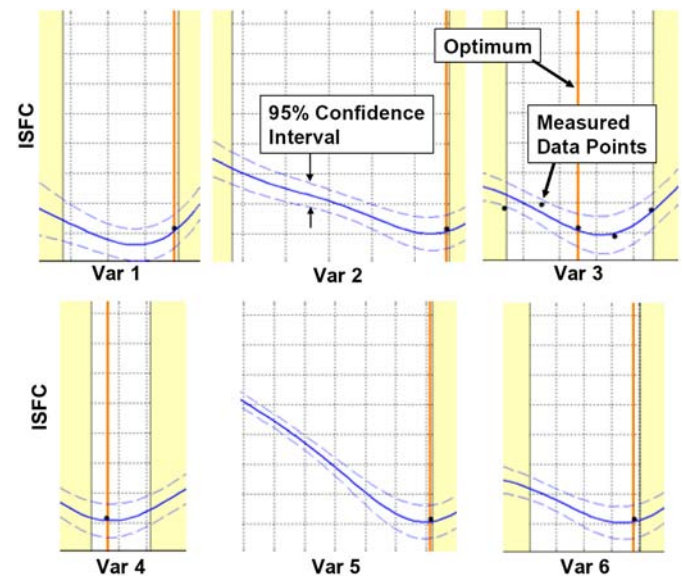


Figure 10. Cross-Section View of RSM for ISFC at Optimum, 1500 RPM, 6 bar IMEP, Triple Injection Strategy

RESULTS: TEST AND ANALYSIS

Test results are shown for part-load operating conditions at 6bar IMEP and 1500 rpm. The engine operating conditions used for most tests are summarized in Figure 11. While emissions targets have not yet been developed for GDCI applications, preliminary targets of FSN<0.5, and ISNO_x<0.2 g/kW-h have been applied. Preliminary constraints for Combustion Noise Level (CNL) of 85 dBA and injection pressure of 500 bar have also been applied, and are shown in Figure 12.

Operating Conditions	
Speed:	1500 rpm
IMEP:	6 bar
Swirl:	Moderate
EGR:	45 %
MAP:	1.8 bar
Pexh:	2.0 bar
Intake Air Temp:	50 C
Coolant, Oil Temp:	90 C
Fuel:	RON 91

Figure 11. GDCI engine test conditions.

Preliminary Emissions Targets and Constraints	
ISNOx	≤ 0.2 g/kW-h
FSN	≤ 0.5
CNL	≤ 85 dBA
Prail	≤ 500 bar

Figure 12. Preliminary emissions targets and Constraints.

Initial tests were performed by injecting gasoline using an unmodified diesel fuel injector. DoE methods described above were applied to determine optimum injection parameters. Results of these initial tests are shown in Figure 13, with ISNOx plotted as function of ISFC. Only points that satisfy the smoke and noise constraint are shown. ISFC values competitive with modern diesel engines were obtained; however, NOx emissions were excessive. It was anticipated that fuel spray characteristics obtained from this injector operating at low fuel pressure with gasoline may be inadequate.

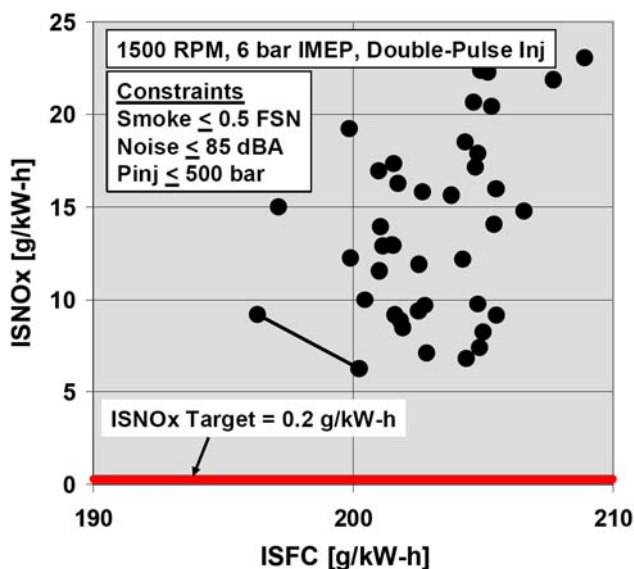


Figure 13. GDCI combustion performance using gasoline in unmodified diesel injector.

A GDCI injection system is being developed for this work. Figure 14 shows the results obtained with a GDCI developmental injector using a single-injection strategy. Single-injection was explored because it offers the advantage of simplified engine calibration. NOx targets can be met at reasonably low ISFC, but noise and smoke targets cannot be met. Either smoke or noise or both smoke and noise are excessive, depending on injection timing. Best results were achieved using high injection pressures of 500 bar.

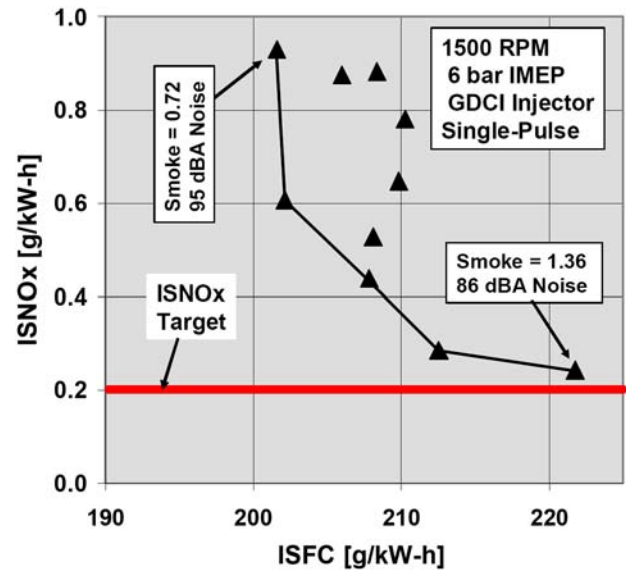


Figure 14. GDCI combustion performance using GDCI injector, single-injection strategy.

Tests were then conducted using double injection strategies. Relative to single injection, fuel consumption for double injection was improved and the NOx target of 0.2 g/kW-h was achieved, while also satisfying smoke and noise constraints. Figure 15 shows a trade-off between ISFC and ISNOx. Also, required injection pressures were reduced.

Tests were also conducted using triple injection. As shown in Figure 15, fuel consumption was further reduced to a minimum ISFC of 181 g/kW-h at an ISNOx of 0.7 g/kW-h. A trade-off between ISFC and ISNOx was also evident. The 0.2 g/kW-h NOx target can be met but with a 7.7 percent fuel consumption penalty. Required injection pressures were also further reduced.

For reference in Figure 15, a diesel test point is also shown. Tests were performed at 800 bar injection pressure using an unmodified diesel injector with double injection over a wide range of EGR and injection timings. Results were optimized to meet the same smoke and noise constraints as GDCI. At these conditions, the diesel tests indicated significantly higher fuel consumption and NOx than GDCI with triple injection.

The lowest fuel consumption for the diesel tests was 195 g/kW-h, but combustion noise was excessive at this condition.

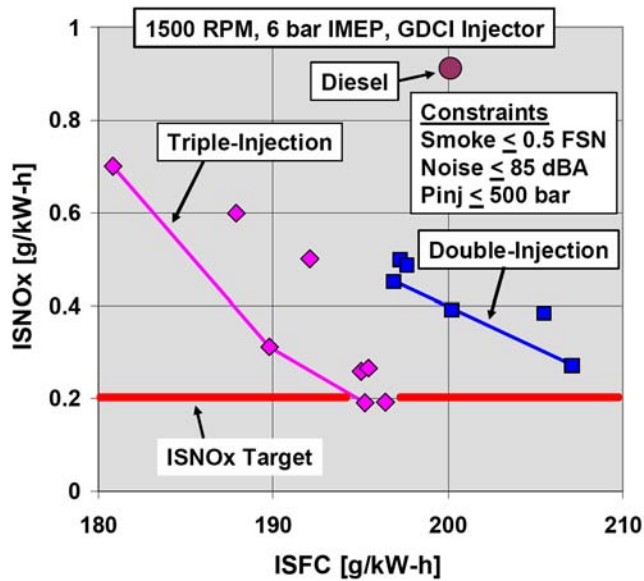


Figure 15. Combustion performance using GDCI injector with double and triple injection strategies.

Detailed heat release analysis was performed for the GDCI tests with the lowest ISFC. Heat release rates and corresponding injector logic pulses are plotted in Figure 16. It is observed that combustion becomes more optimally phased as the injection strategy progresses from single injection to triple injection. Maximum rate of heat release also decreases. In all cases, burn characteristics are well behaved.

A comparison of heat release between the diesel and triple-injection GDCI is shown in Figure 17. The pre-injection of diesel fuel releases heat prior to TDC with some negative work. The phasing of the main heat release is also somewhat retarded relative to the triple-injection GDCI result. These results are consistent with the ISFC data shown in Figure 15.

A portion of the improved fuel consumption of GDCI with triple-injection may be due to reduced cylinder heat transfer. The results from a preliminary energy balance analysis are shown in Figure 18. A large reduction in heat loss during the expansion stroke is observed as injection strategy progresses from single to triple injection. It is surmised that double and triple injection produce a more favorable distribution of fuel during combustion which results in less contact between hot combustion gases and the chamber walls. Heat loss estimates for the diesel are also consistent with the ISFC data shown in Figure 15.

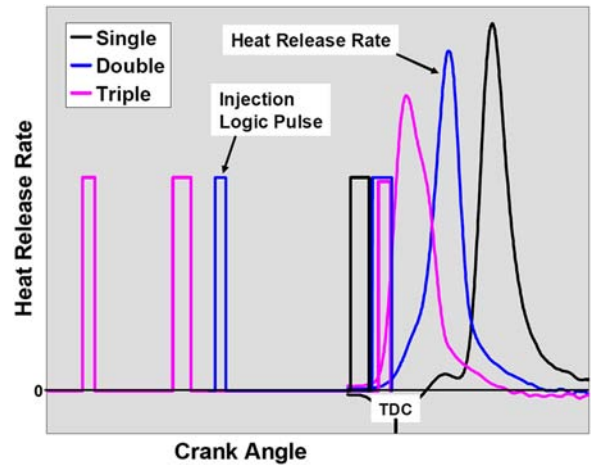


Figure 16. Heat release comparison between Single, Double and Triple Injection Strategies

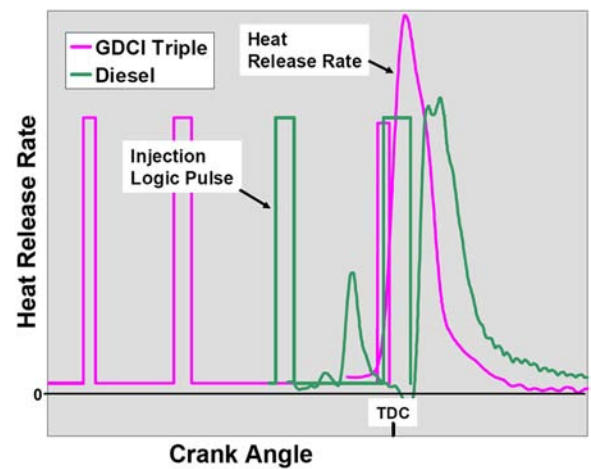


Figure 17. Heat release comparison between Diesel and GDCI Triple Injection Strategy

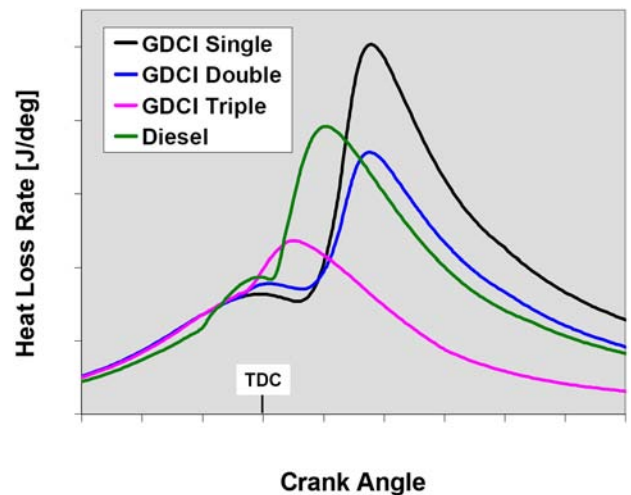


Figure 18. Heat loss comparison.

Combustion and emissions data for single, double, and triple GDCI injection are shown in Figures 19 and 20, respectively. Constraints for CNL and FSN are shown by red horizontal lines. Results are shown for the injection parameters that produce the lowest ISFC, while meeting noise and smoke constraints. For single injection, noise and smoke targets cannot be met simultaneously, so the low noise/high smoke point was chosen for plotting purposes.

As discussed above, triple injection provides the lowest ISFC relative to both single and double injection. This efficiency improvement is obtained partly by enabling more advanced combustion phasing. This provides greater expansion ratio for more of the burned fuel since that fuel burns earlier overall than with single or double injection. For triple injection, very little heat release occurs before TDC.

10-90 burn duration is also shorter for triple injection with significantly higher peak cylinder pressure (PCP). However, CNL are below the 85 dBA constraint with maximum rate of pressure rise (MPRR) in the 5 to 6 bar/CAD range. Importantly, multiple injection enables use of lower injection pressure, which is key to low cost fuel injection system (FIS) and low fuel pump parasitics.

Combustion efficiency (CE) shown in Figure 19 is about 97%, and is slightly higher for triple injection compared to single or double injection. This indicates that a relatively high portion of the injected fuel is being converted to complete combustion products. This CE is commensurate with that measured for typical spark-ignited (SI) engines. While ISHC emissions (Figure 20) are reasonably low, ISCO emissions are higher than desired. CO emissions account for most of the loss of combustion efficiency and may pose challenges for aftertreatment. System level improvements are expected to decrease CO emissions and further increase combustion efficiency through the course of this work.

NOx emissions for GDCI are shown in Figure 20 and increase with the number of injections. More nearly optimum combustion phasing and shorter duration produce higher peak cylinder pressure and temperature. However, from Figures 14 and 15, it is apparent that if operating conditions are chosen to reduce ISNOx to the 0.2 g/kW-h target, the relative ISFC benefit is maintained. Presumably the diesel would suffer a similar ISFC loss. ISCO2 decreases significantly with triple injection as expected from lower ISFC and lower CO emissions. Also as expected, exhaust temperature measured at the exhaust port decreases as ISFC decreases. Depending on the aftertreatment required, these reduced temperatures may or may not be acceptable. More work is needed to understand what engine-out emissions levels can be achieved and what targets are necessary with various applications and aftertreatment technologies.

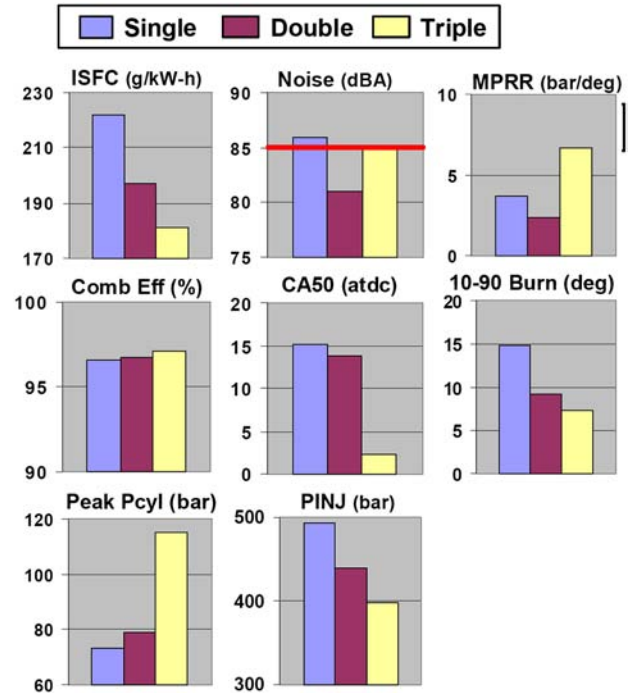


Figure 19. Effect of multiple injection on GDCI combustion.

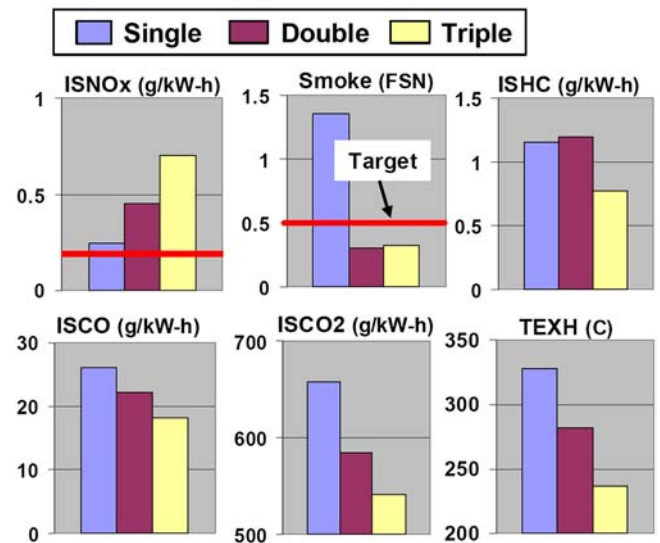


Figure 20. Effect of multiple injection on GDCI emissions.

PRELIMINARY SIMULATION RESULTS

Simulation tools have been used in conjunction with engine testing to understand and improve the GDCI injection process. In this section, preliminary simulation results will be shown for GDCI using triple injection, which produced the lowest ISFC (as shown in Figure 15).

A one-dimensional model of the GDCI injector used in these experiments was developed using AMESim [16]. This model was correlated to the measured injector mean flow obtained during injector calibration, and compared against instantaneous rate-of-injection measurements. The model provides estimated injector lift and internal fuel pressure (Figure 21) that are difficult to measure. Instantaneous injector flow rate and lift are needed as inputs in computational-fluid-dynamic (CFD) simulations of the injection, spray and mixing processes.

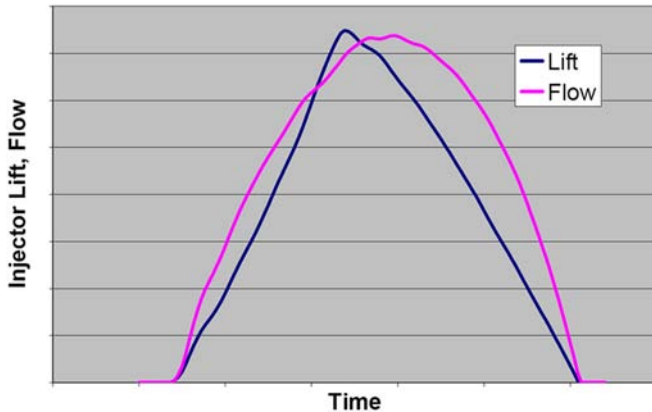


Figure 21. Example: AMESim estimates of instantaneous injector lift and flow for a single injection pulse.

Three-dimensional simulations of the injection, spray, and mixing processes were performed using AVL FIRE software [17]. Detailed geometric data from the test engine and injection system were used in the models. Gasoline fuel properties based on the test fuel were used in the simulation. The simulation commences at intake valve closing (IVC). At this time, in-cylinder conditions including cylinder trapped mass and composition, average temperature, pressure, and initial mixture motion were determined from a combination of engine test data and engine simulation results using GT Power [18].

For the case of GDCI single injection, the fuel is injected as a relatively long, continuous pulse. The simulation results show that even with a properly targeted injector, the relatively long injection pulse causes the spray plume to penetrate to the piston surface. Some fuel hits the piston surface and results in less than ideal mixing. While improved for double injection strategy, the triple injection strategy provides the best results.

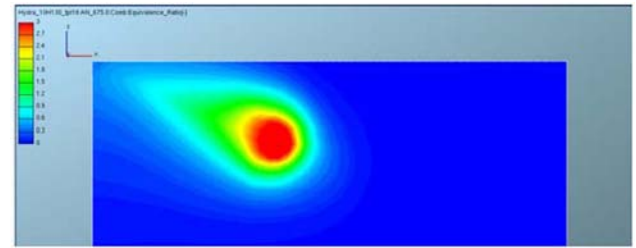


Figure 22. In-cylinder equivalence-ratio contour plot during first injection from FIRE simulation. GDCI triple injection strategy.

Figures 22, 23, 24 show simulation results for triple injection GDCI. Corresponding to first, second, and third injections, respectively, each figure shows a cross-section through the cylinder centerline that is also aligned with one spray plume. In this image sequence, the fuel is delivered in three injection pulses with optimized quantities and separations. The color contours represent the local fuel/air equivalence ratio between 0 and 3.

The first injection (Figure 22) is timed relatively early with the piston positioned well below the TDC position. In this case, the fuel is targeted above the piston bowl and aimed toward the piston top, however the pulse is short enough and fuel vaporization is rapid enough that fuel does not penetrate to the piston or to the cool cylinder walls or topland region. The fuel mixes in the chamber to an overall lean air-fuel ratio. Squish flows are not yet evident.

The second injection is delivered with higher piston position (Figure 23). Targeting is aimed toward the upper piston bowl. Again, since the duration is short and evaporation rates are high, liquid fuel does not reach the piston surface. The second pulse evaporates completely and mixes in the chamber with the first pulse to an overall lean air-fuel ratio. Some evidence of the forming squish flows may be apparent. Due to the autoignition properties of RON91 gasoline, fuel from the first and second injections do not release heat during the compression process prior to the third injection pulse. This is consistent with measured heat release data shown in Figure 16.

Figure 24 shows the third injection. Squish flows are now clearly formed and both aid mixing and help keep fuel out of cool topland and wall regions. With the piston nearly at TDC, fuel is undergoing mixing in the piston bowl. The simulation indicates an absence of fuel puddling on piston surfaces. However, by the end of the third injection event, the fuel-air mixture is stratified.

The “phi-Temperature diagram” is useful to show the local equivalence ratio versus the local temperature across the cylinder as demonstrated originally by Toyota [19] for smoke-less rich combustion. Figure 25 shows the calculated

“phi-T diagram” from simulation corresponding to the state of the mixture during the third GDCI injection. Three different crank positions are shown. This follows the evolution of the fuel and gas mixing process in the cylinder. The labeled NOx and Soot contours on the plot show unfavorable zones.

Figure 25 indicates for the triple injection strategy that injected fuel mixes rapidly with air to form a lean stratified mixture prior to significant heat release. At the start of combustion (SOC), the fuel is stratified but sufficiently mixed with maximum equivalence ratio below the critical level of two, which is needed for low soot emissions. Figure 25 shows that the GDCI injection system provides good mixing-controlled stratification and also produces low NOx, PM, and excellent fuel consumption.

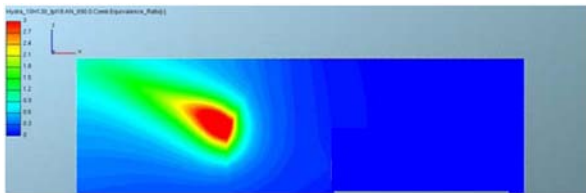


Figure 23. In-cylinder equivalence-ratio contour plot during second injection from FIRE simulation. GDCI triple injection strategy.

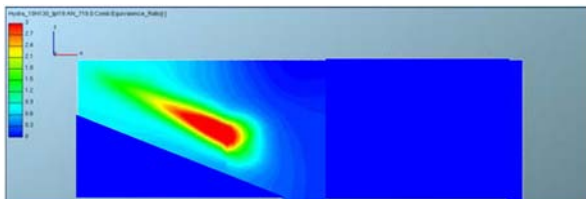


Figure 24. In-cyl. equivalence-ratio contour plot during third injection from FIRE simulation. GDCI triple injection strategy.

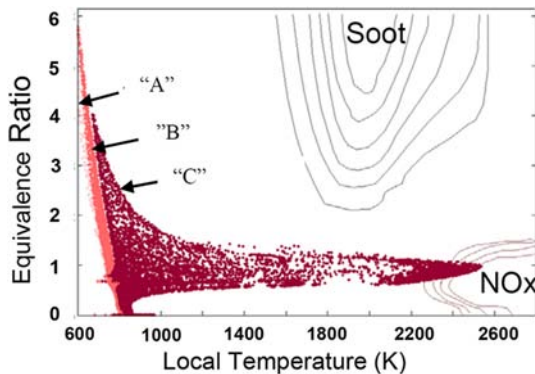


Figure 25. Phi-temperature diagram for three crank angle during third injection from FIRE simulation. GDCI triple injection strategy.

COMPARISON TO OTHER ENGINE TYPES

In this section, triple injection GDCI is compared to diesel and other competitive engine data in the literature.

Figure 26 shows a comparison between GDCI and diesel at the 6 bar IMEP - 1500 rpm test condition reported in this study. The best-ISFC point for triple injection GDCI is compared to the diesel reference point shown in Figure 15. The test data for GDCI and diesel were equally constrained for FSN and CNL. Triple injection GDCI has about 9.5% better mass-specific fuel consumption and about 8% better indicated thermal efficiency than the diesel. However, because the diesel fuel has higher energy density than the gasoline used in these tests (see Table 2), GDCI has lower volumetric-specific fuel consumption than the diesel (4.5 percent). Indicated specific mass CO₂ emissions are shown in the bars on the right side in Figure 26. GDCI has approximately 14 percent lower CO₂ emissions on this basis.

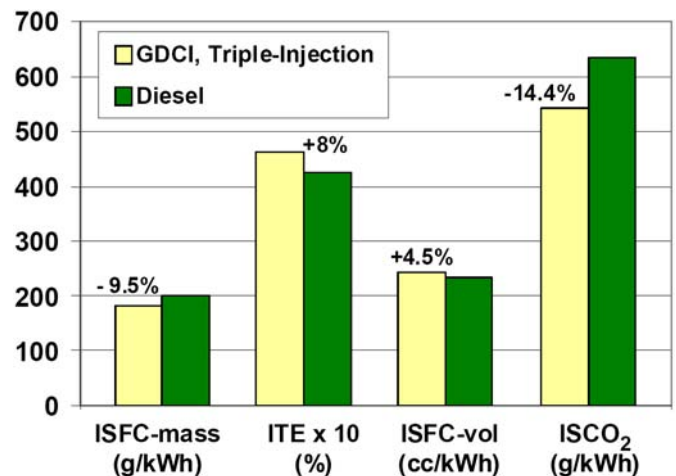


Figure 26. Fuel consumption and CO₂ emissions comparison; triple-injection GDCI vs. Diesel.

Using single-cylinder test results, brake specific fuel consumption (BSFC) for a multi-cylinder GDCI engine was estimated and then compared to data for various engine types available in the literature. The purpose of this comparison was to make a preliminary assessment of the fuel economy potential of GDCI relative to competitive light duty engines. Results are shown in Figure 27.

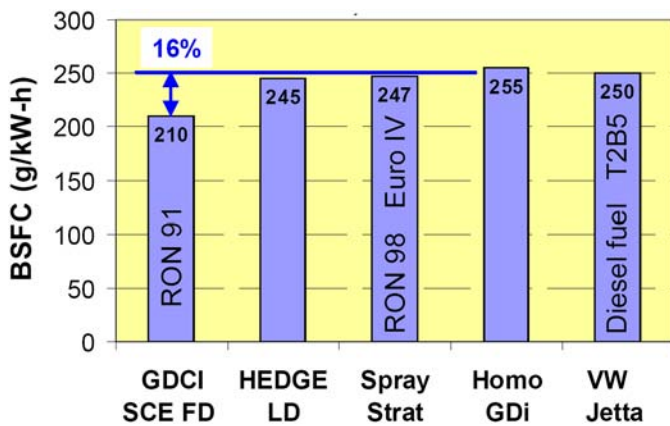


Figure 27. BSFC comparison at 1500 rpm - 5 bar BMEP. GDCI BSFC estimated from single-cylinder engine testing.

The Volkswagen Jetta 2.01 turbodiesel has BSFC of 250 g/kW-h [17]; a homogeneous gasoline direct-injected spark-ignited engine [21] has BSFC of about 255; the Daimler 3.5L V6 spray-stratified engine [22] has BSFC of about 247; and a gasoline spark-ignited engine with increased cooled EGR (HEDGE)[23] has BSFC of about 245 g/kW-h. The estimated BSFC for a multi-cylinder GDCI engine is about 210 g/kW-h or about 16 percent less than the Jetta diesel. This indicates that, at this important part-load operating condition, GDCI has good fuel economy potential. Much work is needed to realize this potential in a practical multi-cylinder engine at regulated emissions levels.

SUMMARY AND CONCLUSIONS

Preliminary single-cylinder engine tests have been conducted at 6 bar IMEP and 1500 rpm using RON91 gasoline to evaluate GDCI injection strategies at low injection pressure. All tests were conducted using Design of Experiments methods. Preliminary optimums were determined using Response Surface Modeling methods and constrained optimization.

It was found that a triple-injection strategy with optimized injection timings and quantities produced the best fuel economy. The triple-injection strategy enabled use of the lowest injection pressures compared to both single-injection and double-injection strategies.

For triple-injection GDCI:

1. A minimum ISFC of 181 g/kW-h was measured. This corresponds to ITE of 46.2 percent. This was about 8 percent more efficient than representative tests of a diesel combustion system running on the same engine. Combustion efficiency was about 97 percent, which is typical of spark-ignited engines.
2. ISNOX of 0.7 g/kW-h and FSN of 0.3 were measured at the minimum ISFC condition with CNL of 85 dBA. A trade-

off between ISFC and ISNOX was observed. In order to achieve the preliminary NOx target of 0.2 g/kW-h, a 7.7 percent fuel consumption penalty was required.

3. ISCO₂ emissions at the minimum ISFC condition were 542 g/kW-h, or about 14 percent less than the diesel baseline.
4. Hydrocarbon emissions were reasonably low (0.75 g/kW-h). This may be expected based on preliminary simulations of the spray and mixing processes. Very little (if any) fuel penetrated to the piston surfaces or the cool cylinder wall regions.
5. Carbon monoxide emissions were somewhat elevated and were attributed to “over-lean” portions of the mixture that were also last to burn. More detailed study of CO emissions mechanisms is needed.

Overall, significant progress has been achieved toward demonstrating the viability of a practical GDCI combustion system. A developmental GDCI injection system exhibited good control of mixture stratification. Injection pressure requirements are much lower than conventional diesel engines but higher than current gasoline direct injection (GDI) engines.

BSFC for a multi-cylinder GDCI engine was estimated based on single-cylinder test results at 6 bar IMEP and 1500 rpm. On this basis, fuel economy potential appears very good compared to competitive power trains. Significant development work is needed to develop a practical GDCI engine system.

REFERENCES

1. Kalghatgi, G., Risberg, P., Angstrom, H-E., “Advantages of a Fuel with High Resistance to Auto-ignition in Late-injection, Low-temperature, Compression Ignition Combustion,” SAE Technical Paper [2006-01-3385](#), 2006, doi:[10.4271/2006-01-3385](#).
2. Kalghatgi, G., Risberg, P., Angstrom, H-E., “Partially Premixed Auto-Ignition of Gasoline to Attain Low Smoke and Low NOx at High Load in a Compression Ignition Engine and Comparison with a Diesel Fuel,” SAE Technical Paper [2007-01-0006](#), 2007, doi:[10.4271/2007-01-0006](#).
3. Kalghatgi, G., et al., “Low NOx and Low Smoke Operation of a Diesel Engine using Gasoline-Like Fuels”, ASME 2009 International Combustion Engine Division Spring Technical Conference, ICES2009-76034, 2009.
4. Kalghatgi, G., “Auto-Ignition Quality of Practical Fuels and Implications for Fuel Requirements of Future SI and HCCI Engines,” SAE Technical Paper [2005-01-0239](#), 2005, doi:[10.4271/2005-01-0239](#).
5. Hansen, R., Splitter, D., and Reitz, R., “Operating a Heavy-Duty Direct-Injection Compression-Ignition Engine

with Gasoline for Low Emissions,” SAE Technical Paper [2009-01-1442](#), 2009, doi:[10.4271/2009-01-1442](#).

6. Kokjohn, S., Hanson, R., Splitter, D., and Reitz, R. “Experiments and Modeling of Dual Fuel HCCI and PCCI Combustion Using In-Cylinder Fuel Blending,” *SAE Int. J. Engines* **2**(2):24-39, 2009, doi:[10.4271/2009-01-2647](#).

7. Ra, Y., Yun, J.E., and Reitz, R., “Numerical Simulation of Diesel Engine Operation with Gasoline,” *Combustion, Science, and Technology*, Vol 181, 2009.

8. Manente, V., Johansson, B., and Tunestal, P., “Partially Premixed Combustion at High Load using Gasoline and Ethanol, a Comparison with Diesel,” SAE Technical Paper [2009-01-0944](#), 2009, doi:[10.4271/2009-01-0944](#).

9. Manente, V., Johansson, B., and Tunestal, P., “Half Load Partially Premixed Combustion, PPC, with High Octane Number Fuels. Gasoline and Ethanol Compared with Diesel”, SIAT 2009 295, 2009.

10. Manente, V., Johansson, B., and Tunestal, P., “Characterization of Partially Premixed Combustion with Ethanol: EGR Sweeps, Low and Maximum Loads”, ASME International Combustion Engine Division 2009 Technical Conference, ICES2009-76165, 2009.

11. *Labview RT Software*, Release 2009, National Instruments, Austin, TX

12. Drivven, Inc., San Antonio, TX

13. Sinnamon, J., and Sellnau, M., “A New Technique for Residual Gas Estimation and Modeling in Engines,” SAE Technical Paper [2008-01-0093](#), 2008, doi:[10.4271/2008-01-0093](#).

14. Sellnau, M., Sinnamon, J., Oberdier, L., Dase, C., et al., “Development of a Practical Tool for Residual Gas Estimation in IC Engines,” SAE Technical Paper [2009-01-0695](#), 2009, doi:[10.4271/2009-01-0695](#).

15. *Model-Based Calibration Toolbox™* Version 4.1, MathWorks Release 2010B, August 16, 2010

16. *AMESim Software*, Version 8, LMS International, 2010.

17. *AVL FIRE Software*, Version 2009, AVL Advanced Simulation Technologies, Graz, Austria.

18. *GT Power Software™*, Version 7.0, Gamma Technologies, Inc., Westmont, Illinois, 2010.

19. Akihama, K., Takatori, Y., Inagaki, K., Sasaki, S., Dean, A., “Mechanism of Smokeless Rich Diesel Combustion by Reducing Temperature,” SAE Technical Paper [2001-01-0655](#), 2001, doi:[10.4271/2001-01-0655](#).

20. Hadler, J., et al., “Volkswagen's New 2.0l TDI Engine Fulfills the Most Stringent Emissions Standards,” 29th Vienna Motor Symposium, 2008.

21. Yu, C-H., Park, K., Han, S., Kim, W., “Development of Theta II 2.4L GDI Engine for High Power and Low

Emissions,” SAE Technical Paper [2009-01-1486](#), 2009, doi:[10.4271/2009-01-1486](#).

22. Luckert, P., et al., “The New V6 Gasoline Engine with Direct Injection by Mercedes-Benz,” *MTZ* 11/2006 Vol 67, 2006.

23. Alger, T., Gingrich, J., Roberts, C., and Mangold, B. “Cooled EGR for Fuel Economy and Emissions Improvement in Gasoline Engines,” JSAE Paper 20105013, JSAE Annual Congress, 2010.

CONTACT INFORMATION

Mark Sellnau
Engineering Manager
Delphi Advanced Powertrain
3000 University Drive
Auburn Hills, MI 48326
mark.sellnau@delphi.com

ACKNOWLEDGEMENTS

The authors gratefully acknowledge contributions to this work from Dan Trytko and Jeffery Webb (Delphi test engineers); Tim Kunz at Delphi Powertrain; Philip Dingle and Delphi Diesel Systems in Gillingham, England and Blois, France; Choi-bum Kweon at the US Army Research Office (formerly Delphi); Professor Rolf Reitz, Professor Chris Rutland, and Harmit Juneja of Wisconsin Engine Research Consultants (WERC); Professor Jaal Ghandhi at Engine Research Center (ERC) University of Wisconsin-Madison; Professor Gautam Kalghatgi at Shell Global Solutions, UK.

ACRONYMS

Parameter	Units	Description
BSFC	g/kW-h	Brake specific fuel consumption
CAD	degrees	Crank angle degrees
CE	percent	Combustion efficiency
CFD		Computational Fluid Dynamics
CNL	dba	Combustion Noise Level
CO	g/kW-h	Carbon monoxide emissions
DoE		Design of Experiments
EGR	percent by mass	Exhaust gas recirculation
FIS		Fuel injection system
FSN		Filtered Smoke Number
GDCI		Gasoline Direct Injection Compression Ignition
HC	g/kW-h	Hydrocarbon emissions
HCCI		Homogeneous Charge Compression Ignition
IMEP	bar	Indicated Mean Effective Pressure
ISCO	g/kW-h	Indicated specific carbon monoxide emissions
ISCO2	g/kW-h	Indicated specific carbon dioxide emissions
ISFC	g/kW-h	Indicated specific fuel consumption
ISHC	g/kW-h	Indicated specific hydrocarbon emissions
ISNOx	g/kW-h	Indicated specific nitrous oxide emissions
IVC	CAD	Intake valve closing
MBC		Model Based Control
PCP	bar	Peak cylinder pressure
PDA		Port Deactivation
PID		Proportional, Integral, Derivative Controller
Prail	bar	Rail Pressure
PW	ms	Pulse Width
Q	mm ³	Quantity injected
Q%	percent	Quantity injected as percent of total fuel
RON		Research Octane Number
RPM		Revolutions per minute
RSM		Response Surface Modeling
SI		Spark ignited
SOI	CAD btdc	Start of Injection
TDC		Top dead center

The Engineering Meetings Board has approved this paper for publication. It has successfully completed SAE's peer review process under the supervision of the session organizer. This process requires a minimum of three (3) reviews by industry experts.

All rights reserved. No part of this publication may be reproduced, stored in a retrieval system, or transmitted, in any form or by any means, electronic, mechanical, photocopying, recording, or otherwise, without the prior written permission of SAE.

ISSN 0148-7191

Positions and opinions advanced in this paper are those of the author(s) and not necessarily those of SAE. The author is solely responsible for the content of the paper.

SAE Customer Service:

Tel: 877-606-7323 (inside USA and Canada)

Tel: 724-776-4970 (outside USA)

Fax: 724-776-0790

Email: CustomerService@sae.org

SAE Web Address: <http://www.sae.org>

Printed in USA